Woven Model Based Geometric Design of Elastic Medical Braces

Charlie C.L. Wang Kai Tang

***Abstract*—This paper presents an algorithm for automatically computing the planar patterns of custom-made assistive medical braces, which are employed to restrict the motion of the joints (such as wrist and knee) that suffer from musculoskeletal disorders caused by repetitive strain injuries. An elastic brace is manufactured by warping a planar elastic fabric pattern. With a specified material, different shapes of planar patterns for producing a brace will generate different biomechanical effects on the joint. As an assistive medical device, an elastic brace is often requested to provide certain normal pressures at certain specific locations on the joint. Traditionally the planar pattern of a brace respecting the prescribed normal pressure requirement is designed through empirical tests by trial-and-error. We develop a woven fitting based method in this paper to automate this geometric design process.**

***Index Terms*—Geometric modeling, health care, surface flattening, woven model, developability.**

1. INTRODUCTION

REPORTS have shown that more than seven million physician office visits per year in the United States are related to problems with wrist joints suffering from the repetitive strain injury [1]. If other types of joint injury (e.g., sports related) were included, the number would become much bigger. The dramatic increase in the use of computers and various kinds of automatic equipments is, unfortunately, a major contributor to this spate. Elastic braces are the most commonly used assistive medical devices for joint injuries, whose purpose is to restrict the motion of the injured joint so that it will eventually heal by itself. A same brace, however, will exert different biomechanical effects on different individuals since they have different joint shapes. Therefore, for better and faster treatment of an individual patient, more and more physicians now request custom-made braces specifically designed for the individual patient, rather than choosing from off-shelf and mass-produced ones.

A brace is made of a piece of elastic fabric with certain material characteristics. To restrict the motion of the joint, the brace should be in a "positive tensile" state – it must be stretched so that normal pressure can be generated upon the joint. The design task of a brace is to find a planar pattern/geometry of the brace, which is called the "rest or relaxed state" as no stretch or compression occurs at this time, so that when worn the brace generates the desired normal pressure distribution. In most cases (though not every), the planar pattern is sewed at two matching seams so to form a relaxed closed cylinder-like shape. Figure 1 shows such an elbow brace.

Fig. 1. An elbow brace in its normal state (i.e., when worn) – left, and in the rest state – right.

The main component in the design of a brace is to find the correct planar pattern of the flattened brace so that, when worn, the stretched brace will generate the requested distribution of the normal pressure on and near the joint. Currently this flattening is determined manually through a tedious and very inefficient trial-and-error process: markers are placed on the sample points in an initial guess pattern, the corresponding brace is then worn by the patient or put on a cast model of the joint; normal pressure is then measured at some key sample points, and the boundaries of the pattern (the matching seams) are adjusted in an ad-hoc manner by looking at the movements of the markers and the errors of the normal pressure. The research presented in this paper is motivated by this – we develop a computer system that can automate this design process. Specifically, given the material characteristics of the brace, the geometry of the local body shape near the joint where the brace is to be worn, and the desired normal pressure at some designated points on the joint, the presented computer program will output the correct corresponding *flattened* planar pattern of the brace.

We focus on developing a woven model based fitting and flattening algorithm for 3D freeform surfaces, because in the majority of cases braces are made of woven-like materials and human body near the joints exhibits sculpture nature. Fig.2 shows an example that illustrates our flattening algorithm. After obtaining the scanned 3D triangular mesh model of the surface on which the brace is to be put (there exist several commercial

Charlie C.L. Wang is with the Department of Automation and Computer-Aided Engineering, The Chinese University of Hong Kong, Shatin, N.T., Hong Kong, P. R. China (Corresponding Author; phone: 852-2609-8052; fax: 852-2603-6002; e-mail: cwang@acae.cuhk.edu.hk).

Kai Tang is with the Department of Mechanical Engineering, The Hong Kong University of Science and Technology, Clear Water Bay, Kowloon, Hong Kong, P. R. China. (e-mail: mektang@ust.hk).

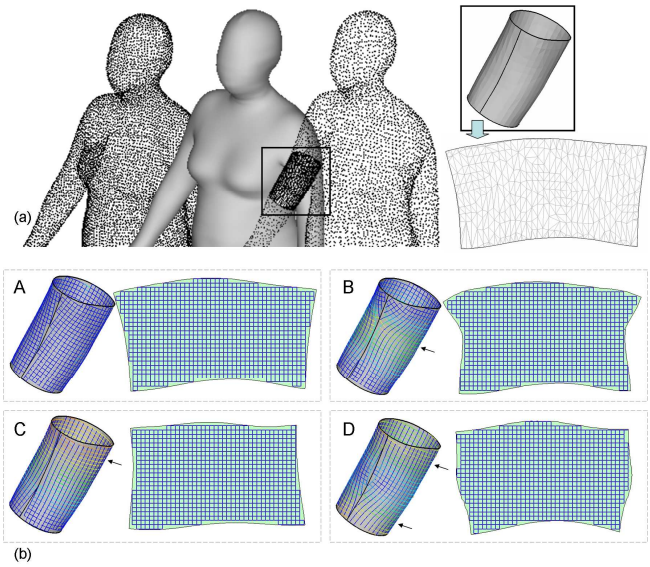

Fig. 2. Geometric design of a customized assistive medical brace: (a) the 3D mesh surface of the brace is acquired from a scanned human model, and the initial planar pattern is obtained by a parameterization algorithm [5]; (b) different planar patterns are computed by fitting a woven model on the 3D brace surface while satisfying different user specified normal pressure requirements – different colors on the 3D brace represent different strain levels with blue denoting zero and red the highest value (=0.25). The places pointed by arrows are with large normal pressures specified.

products for this data acquisition task, e.g., [2], [3], and [4]), an initial 2D pattern of the brace can be determined by the well-known mesh parameterization algorithm in [5] (see Fig.2(a)). Based on this initial pattern, a woven model is then fit onto the 3D mesh surface of the brace (shown in the top-left of Fig.2(b)). The next step, which is the main part of the algorithm, is to redistribute the woven nodes on the 3D mesh surface (including possible insertion and removal of some nodes) so that the required normal pressures at the specified points are satisfied. To accomplish this, we first establish the relationship between the normal pressure and the strains of the woven model on the surface, and then convert the node-distribution problem into a strain-energy minimization problem and solve it through a diffusion process. Figure 2(b) shows several resultant patterns of a given 3D brace shape based on different user assigned normal pressures.

The major contributions of our work fall in two aspects:

- A mathematical model is established that relates the woven strains of a brace to the normal pressure that the brace generates on a freeform surface.
- We develop an algorithm which, given the geometry of the freeform surface and the prescribed normal pressure, computes the corresponding 2D pattern of the brace. No such algorithm is found in literature.

The result of this research will change the current inefficient trial-and-error manner in the design and fabrication of custom-made assistive medical braces, and provide a useful computer-aided design tool for physicians. In addition, the methodology developed can also benefit many other industrial applications that have similar surface flattening problems, e.g., the shoe industry, the apparel industry, and the furniture industry, etc. The relevance of applying our current method to those applications depends on whether the assumptions given in section 3 fulfill the physical characteristics there.

The paper is organized as follows. The next section reviews the related works in literature. In Section 3, we introduce the woven mesh mode. In Section 4, we first present the methodology about how to relate the normal pressure to the strains of a woven mesh model, followed by the general idea of the corresponding flattening algorithm. The implementation detail of the algorithm is provided in Section 5. Finally, we show several numerical computation results in Section 6, and then conclude the paper.

2. Literature Review

The related works done by others are reviewed below in several integral subjects. A recent work directly pertinent to design of braces was given in [6]. In that work, the authors employed a strain energy density function to compute the stiffness that could be generated by an elastic brace during the deflection of human joints. Different from theirs, which is forward analysis, the objective of our research is to seek a solution to the reverse problem (i.e., the backward synthesis): given some biomechanical parameters (i.e., the strain distribution or the desired normal pressures at some sample points), compute the planar pattern of the brace which will generate that strain distribution on the specific individual.

As to be detailed in the *methodology* section, the core part of our proposed approach is a delicate algorithm that flattens a freeform surface with a prescribed tensile strain distribution into its corresponding relaxed planar pattern. The amount of work that has been done in this general area of surface flattening is immense. It is usually formulated as the surface development problem in design/manufacturing applications and the mesh parameterization problem in computational geometry and computer graphics community. Regardless of the targeted applications, all the past works in surface flattening share a common goal: establish a mapping between a given surface and a planar region with minimum area and angular distortion. An excellent survey of recent advance in mesh parameterization is given in [7]. Floater [8] introduced a graph-theory based parameterization for tessellated surfaces for the purpose of smooth surface fitting; his parameterization (actually a planar triangulation) is the solution to a linear system based on convex combination. A quasi-conformal parameterization method based on a least-squares approximation of the Cauchy-Riemann equations was given in [9], where the objective of minimization is angle deformation. Desbrun et al. [5] developed an efficient parameterization algorithm for minimizing the distortion of different intrinsic measures of the original mesh. In all the above works, however, pre-existing linear stretch on the original surface is not considered.

In the realm of texture mapping which is a special application of surface flattening, Sheffer and de Sturler [10, 11] gave a texture mapping algorithm that incurs low mapping distortion. In [12], a texture stretch metric was introduced to minimize the linear distortion via non-linear optimization. Since non-linear numerical optimization is conducted in both, these approaches are time consuming. More recently, in [13], a fast and simple method for generating a low-stretch mesh parameterization was presented. It starts from any other parameterization (e.g., the intrinsic parameterization [5]) and then improves the parameterization gradually by a diffusion process using the stretch metric of [12]. It can significantly lower the stretch in a mesh parameterization. However, since the boundary vertices are not moved, the 2D boundary profile depends on the initial parameterization. Since in [5] the stretch is not minimized, the resultant 2D profiles of [13] are seldom satisfied in the length or area requirement.

There are also some other energy-minimization based flattening algorithms [14-19]. All these algorithms though share a common "backward" strategy: the energy minimization scheme is applied to the 2D pattern. In other words, they assume that the original 3D surface has zero energy, i.e., without compression or stretch, while the 2D pattern is sought that minimizes the deformation energy. On the contrary, most physical processes are just opposite, such as in our case where the original 3D surface is the shape of the brace in normal state which is required to have a non-zero stretch distribution.

In the majority of situations, braces are made of woven materials. Woven fabrics consist of a series of vertical threads (weft) that cross with a series of horizontal threads (warp). (The two though can intersect at a non-right angle.) In this sense, our proposed method relates to the work presented in [20-22], where Aono et al. proposed a geometrical approach for flattening a woven ply. We recently presented a flattening algorithm in [23] for woven fabrics. Our algorithm adopts a strain-energy releasing process and employs the idea of geodesic path, which partially solved the problems encountered by Aono et al.'s methods [20-22]. However, as aforementioned, none of the above approaches consider the prescribed normal pressures or tensile strain distributions when flattening freeform surfaces. This is the problem to be solved in this paper.

3. Woven Model for Elastic Brace

The geometric design of a user-customized elastic medical brace is in fact based on the simulation of stretching a woven model onto a freeform polygonal mesh surface M which represents the 3D shape of the joint. Therefore, we need first to define the woven model.

A brace can be regarded as a ply of woven fabric composed of horizontal and vertical threads interwoven in a specific fashion (e.g., the one shown in Fig.3(a)). From the study of materials [24], we can adopt the following definitions and assumptions on the ply for an elastic brace:

Assumption 1 All the weft threads are fabricated with a same type of material, and hence with a constant tensile stiffness coefficient. The same is true for all the warp threads.

Assumption 2 The ply generally has strong tensile-strain resistance in the thread direction and a much weaker shear-strain resistance.

Assumption 3 No slippage occurs at the crossing of a weft (vertical) and a warp (horizontal) thread.

Assumption 4 To simplify the physical model, the frictions – both the friction between threads and the friction between the woven fabric and the surface wearing the brace – are ignored.

TABLE 1 Nomenclature

Symbol	Meaning
M	A given polygonal mesh surface
Γ	A spring mesh to model the woven models
P_V	Normal pressure at a woven node V
κ_H	Mean curvature at a surface point
σ	Stress
ε	Strain
L_S	The length of a spring S
k_{warp} , k_{weft} , k_{diag}	The stiffness coefficients of warp, weft and diagonal springs
$V_{i,j}$	Woven node with index (i, j)
λ	A damping factor in diffusion-based energy minimization
E_{SSD}	The squared strain difference

Based on the above, in our approach, the woven fabric is modeled by a spring mesh Γ. An example spring mesh model is shown in Fig.3(b). There are three components in this model, i.e., weft (vertical) springs, warp (horizontal) springs, and diagonal springs. For real woven fabric, there is no diagonal thread in general. The reason for adding diagonal springs is to simulate the shear deformation resistance. Each of the three types of the springs has its own initial length at which the spring attains zero energy. A *woven node* is an intersection between springs whose position determines the deformation of the springs connected to that node. Each node is indexed by $V_{i,j}$, where i, j are integers representing the indexes of row and column, respectively. For a mesh node $V_{i,j}$, its valence is the number of springs connecting to it. If the valence is eight, $V_{i,j}$ is an *internal node*; otherwise, $V_{i,j}$ is called a *boundary node*. For a mesh node $V_{i,j}$, if there is another mesh node $V_{i+a,j+b}$ satisfying: 1) $a,b \in \{-1,0,1\}$ and 2) $|a|+|b|>0$, $V_{i+a,j+b}$ is called a *neighboring node* of $V_{i,j}$. For a woven mesh in 2D, all the weft springs are aligned in one direction and all the warp springs are aligned in another direction. In our model, their

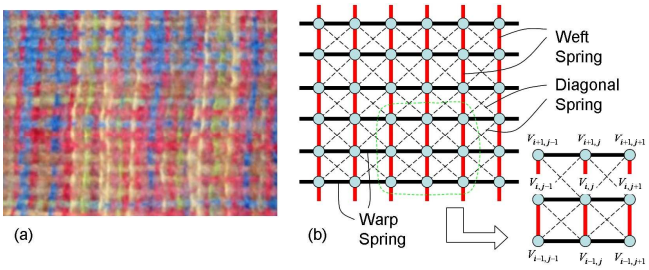

Fig. 3. Woven model: (a) a piece of real woven fabric; (b) our spring mesh representation of a piece of woven fabric.

directions are orthogonal to each other, although they don't have to. If the initial length of the weft spring and the warp spring are L_{weft} and L_{warp} respectively, the initial length of the diagonal spring r_{diag} is given by

$$L_{diag} = \sqrt{L_{weft}^2 + L_{warp}^2}\ .$$

Lemma 1 Anisotropic material properties can be achieved by assigning different spring stiffness coefficients k_{weft}, k_{warp} and k_{diag} to the weft, the warp, and the diagonal springs.

Note that by Assumption 1, all weft springs should have the same stiffness coefficient. The same are the warp and the diagonal springs. Also, by Assumption 2, we have Lemma 2 below.

Lemma 2 In general, $k_{diag} << k_{weft}$ and $k_{diag} << k_{warp}$.

Since no slippage occurs at a woven node (by Assumption 3) and the frictions are neglected (by Assumption 4), the forces generated at the two warp springs linked to a particular woven node should be equal to each other – this is also true for the weft springs. Since, due to Lemma 2, the forces contributed by diagonal springs are extremely small, they can be ignored in our model when formulating the relationship between normal pressures and tensile strains. However, the function of diagonal springs cannot be ignored when releasing elastic energy on the woven model (will be introduced in section 4.3), where they prevent the woven mesh from being overlapped. We thus have the following lemma.

Lemma 3 When in equilibrium, the strain on a single weft or warp thread is a constant.

The planar woven mesh Γ can be easily fitted onto the 3D freeform surface M, if we have determined a planar parameterization Ω of M. For a woven node $V_{i,j} \in \Gamma$, suppose it falls in a triangle $T_k \in \mathrm{M}$ on Ω. We compute the barycentric coordinate of $V_{i,j}$ in T_k on Ω. After applying the same barycentric coordinate on the same triangle T_k in 3D, we have mapped $V_{i,j}$ onto the 3D freeform surface M. By this mapping method, every woven node is on the freeform surface precisely. However, the directions and lengths of different kinds of springs may not be preserved as compared to their 2D counterparts. This leads to strains – so that normal pressure is generated on M. The objective is to find a correct Ω that satisfies the prescribed normal pressures at some specified points.

4. METHODOLOGY

In this section, we present the main methodology for computing the planar pattern of a brace that satisfies prescribed normal pressures at certain specified points.

4.1. *Normal pressure and tensile strain*

The purpose of an assistive medical brace is to exert normal pressure on the joint. This is jointly accomplished by the tensile strain (stretch) of the brace and the curvature of the joint-surface[1]. To a physician, only the normal pressure is meaningful, which though must be converted to tensile strain for our use. The general relationship between the two has not been explored before. However, motivated by the theories of solid mechanics [25], we stipulate that it can be reasonably modeled as

$$P_n = f\left(\int_0^{2\pi} g(\kappa(\theta)) \cdot \sigma(\theta) d\theta\right)$$

where both $f(\cdots)$ and $g(\cdots)$ are some positive and monotone scalar functions, $\kappa(\theta)$ represents the normal curvature in direction θ on the tangent plane at the surface point, and $\sigma(\theta)$ denotes the normal stress in θ. Without loss of generality, the value of the normal pressure at a woven node V on M can be computed by the formula

$$P_V = s\int_0^{2\pi} \kappa_n(\theta)\sigma(\theta) d\theta$$

where s is a coefficient related to the thickness and the material of fabrics of the brace that can be determined through some material tests. Since the material tests exceed the scope of our paper, we simply set s to one in all our numerical tests. We then further simplify the equation to

$$P_V \approx s\int_0^{2\pi} \kappa_H \sigma(\theta) d\theta \qquad (1)$$

by replacing $\kappa_n(\theta)$ with the mean curvature κ_H at this surface point on M. The mean curvature at a point on the polygonal mesh surface can be computed by the method in [26]. Stimulated by the quadratic polynomial

$$z(x, y) = a + by + cy + dx^2 + exy + fy^2$$

which is widely used in discrete differential geometry and geometry processing for interpolating/approximating certain characteristics (e.g., surface normal, curvatures) at a surface point, here we adopt a similar form to represent $\sigma(\theta)$ but replace (x, y) by $(\cos\theta, \sin\theta)$ since $\sigma(\theta)$ is only in terms of an angle θ between the direction and the warp thread on the tangent plane. Thus, the function $\sigma(\theta)$ is represented in the form

[1] Notice that no normal pressure can be generated upon a flat surface no matter how stretched the brace is.

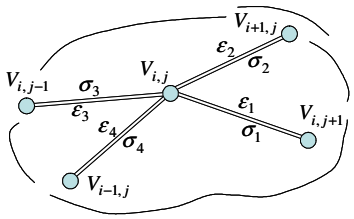

Fig. 4. Stresses and strains on woven springs around a woven node.

$$\sigma(\theta) = a\cos\theta + b\sin\theta + c\cos^2\theta + d\sin^2\theta .$$

For a woven node $V = V_{i,j}$, the stress function is assumed to interpolate the four stresses shown on its adjacent warp and weft springs (see Fig.4), i.e.

$$\sigma(0) = \sigma_1,\ \sigma(\frac{\pi}{2}) = \sigma_2,\ \sigma(\pi) = \sigma_3,\ \sigma(\frac{3\pi}{2}) = \sigma_4 .$$

This interpolation simplification is valid if the density of woven grid is high, which is assumed in our case. By Lemma 2, here we simply neglect the diagonal springs, since their stiffness is generally much smaller than that of warp and weft springs. Therefore, we have

$$a = \frac{\sigma_1 - \sigma_3}{2},\ b = \frac{\sigma_2 - \sigma_4}{2},\ c = \frac{\sigma_1 + \sigma_3}{2},\ \ d = \frac{\sigma_2 + \sigma_4}{2}$$

which yields

$$P_V \approx s\int_0^{2\pi} \kappa_H \sigma(\theta) d\theta = \frac{s\pi\kappa_H}{2}(\sigma_1 + \sigma_2 + \sigma_3 + \sigma_4) .$$

Since

$$\sigma_1 = k_{warp}\varepsilon_1,\ \sigma_2 = k_{weft}\varepsilon_2,\ \sigma_3 = k_{warp}\varepsilon_3,\ \sigma_4 = k_{weft}\varepsilon_4,$$

the normal surface pressure at V can be expressed as

$$P_V \approx \frac{s\pi\kappa_H}{2}(k_{warp}(\varepsilon_1 + \varepsilon_3) + k_{weft}(\varepsilon_2 + \varepsilon_4)) \qquad (2)$$

with

$$\varepsilon_1 = \frac{\left\|V_{i,j}V_{i,j+1}\right\| - L_{warp}}{L_{warp}},\ \varepsilon_2 = \frac{\left\|V_{i,j}V_{i+1,j}\right\| - L_{weft}}{L_{weft}},$$

$$\varepsilon_3 = \frac{\left\|V_{i,j}V_{i,j-1}\right\| - L_{warp}}{L_{warp}},\ \varepsilon_4 = \frac{\left\|V_{i,j}V_{i-1,j}\right\| - L_{weft}}{L_{weft}} .$$

As mentioned above, L_{weft} and L_{warp} are the initial (relaxed) length of the weft springs and the warp springs respectively.

4.2. *Strains on threads*

We have formulated the relationship between the normal pressure and the tensile strength. The next step is to further relate them to the tensile strains on woven springs, since they directly relate to the positions of nodes on the surface. As the woven fitting result must be in an equilibrium state, by Lemma 3, we have $\varepsilon_1 = \varepsilon_3 = \varepsilon_{warp}$ and $\varepsilon_2 = \varepsilon_4 = \varepsilon_{weft}$. Thus, Eq.(2) becomes

$$P_V \approx s\pi\kappa_H(k_{warp}\varepsilon_{warp} + k_{weft}\varepsilon_{weft})$$

For a given P_V, if ε_{weft} is known, the above equation gives the required tensile strain on the warp springs at V. From preliminary physical experiments, we find that the weft strains on medical assistive braces are usually extremely small. Limited by the geometry of various medical assistive braces, the strains on weft threads are mainly generated by the friction between a brace and the human skin. Since the friction is neglected (due to Assumption 4), we have the following Lemma.

Lemma 4 When in equilibrium, the strains on all the weft springs are assumed to be a near-zero constant, $\varepsilon_{weft} \approx 0$.

For any row of woven warp springs on Γ, if there are in total m constraints (normal pressures) assigned on this thread, the desired tensile strain ε_{warp} can be determined by the least-squares fitting with the objective function

$$J_{\varepsilon_{warp}} = \sum_{V=1}^{m}(s\pi\kappa_{H_V}(k_{warp}\varepsilon_{warp} + k_{weft}\varepsilon_{weft}) - P_V^0)^2 .$$

Letting $\partial J_{\varepsilon_{warp}} / \partial \varepsilon_{warp} \equiv 0$, we have

$$\varepsilon_{warp} = \sum_{V=1}^{m}(P_V^0\kappa_{H_V} - s\pi\kappa_{H_V}^2 k_{weft}\varepsilon_{weft}) \Big/ \sum_{V=1}^{m}(s\pi\kappa_{H_V}^2 k_{warp}) \qquad (3)$$

where κ_{H_V} is the mean curvature of the surface M at the position of the woven node V, and P_V^0 is the user specified normal pressure.

There are two critical issues here. First, Eq. (3) works only when the positions on M of all the nodes of the warp thread are known. Second, if a warp thread does not pass through any point on M with a prescribed normal pressure, we still need to calculate its tensile strain ε_{warp}. For the first, we will perform a strain-energy minimization to place all the warp threads on M. For the second, we introduce a smooth curve $\varepsilon(t)$, called the *warp strain distribution function*, to interpolate those tensile warp strains determined by Eq.(3), where t is the parameter in the range [0, 1] corresponding to the row indices of the threads. The warp strains on those threads without normal pressure constraints are given by $\varepsilon(t)$. Besides meeting the prescribed normal pressure requirement, function $\varepsilon(t)$ should also satisfy certain endpoint constrains (e.g., $\varepsilon'(0) = 0$ and $\varepsilon'(1) = 0$).

4.3. *Elastic energy due to strains*

Based on Eq. (2) and (3), we now must place warp threads properly on M so that the prescribed normal pressure can be achieved. We model this in the framework of elastic energy minimization. For a given woven model Γ, the embedded elastic energy is formulated as

$$J_E = \sum_{S\in\Gamma}\frac{1}{2}k_S\left(\left\|V_\alpha V_\beta\right\| - L_S\right)^2 \qquad (4)$$

where V_α and V_β are the woven nodes for a spring $S \in \Gamma$. The constant k_S is one of the spring constants k_{warp}, k_{weft}, or k_{diag}, depending on the type of spring S, and L_S is the rest length of S. The value of J_E depends on the position of woven nodes on M; when randomly moving a woven node on the given surface M, J_E will be changed. When J_E=0, it

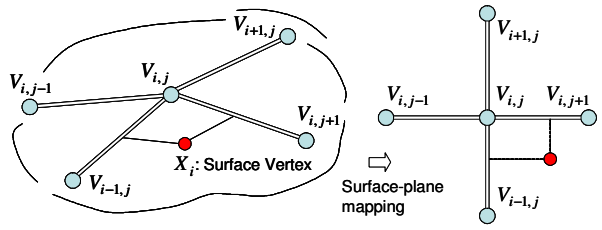

Fig. 5. Interpolated surface-plane mapping.

means that every spring $S \in \Gamma$ now satisfies its rest length L_S. However, due to some constraints (e.g., the given geometry shape), zero J_E usually cannot be achieved. Therefore, a J_E with minimal value is desired. As aforementioned, the initial 3D fitting of the woven model Γ on M can be obtained by any mesh parameterization (e.g. that of [8]) of the given 3D mesh surface M. In general, the lengths of springs on M will not be the same as its rest length in 2D (i.e., L_{weft}, L_{warp}, or L_{diag}). Therefore, J_E can be minimized by moving the woven nodes on M, through a diffusion process (the detail will be given in Section 5. The upper-left figure in Fig.2(b) shows such an example of stretch-free energy minimization.

However, it is imperative to note that, when $L_S = L_{warp}$, L_{weft} or L_{diag}, minimizing the elastic energy J_E will not yield a woven fitting preserving the desired strains per Eq. (3). Therefore, we need to modify the energy function. For a spring S with a prescribed tensile strain ε_S, the desired length of S on M is changed to

$$L_S = (1+\varepsilon_S)L_{warp} \tag{5}$$

for a warp spring, and

$$L_S = (1+\varepsilon_S)L_{weft} \tag{6}$$

for a weft spring. For a diagonal spring linking two warp springs and two weft springs, the expected 3D length of the diagonal spring is computed by

$$L_S = (((1+\bar{\varepsilon}_{warp})L_{warp})^2 + ((1+\bar{\varepsilon}_{weft})L_{weft})^2)^{1/2} \tag{7}$$

where $\bar{\varepsilon}_{warp}$ is the average of the strains on the two warp springs, and $\bar{\varepsilon}_{weft}$ is the average of the strains on the two weft springs. Substituting Eqs. (5-7) into Eq. (4), the minimization of J_E then will give rise to the distribution of the woven nodes on M satisfying the spring strains that will respect the prescribed normal pressure.

4.4. *Surface-plane mapping*

The result of the minimization of J_E (Eq. (4)) is a mapping between the nodes on surface M and their counterparts in the plane. This mapping is discrete since only nodes are mapped. We however need a continuous mapping between M and its corresponding planar pattern. The discrete mapping thus needs to be interpolated so that it becomes continuous – every point on M has its counterpart defined in the plane.

Our interpolation scheme is akin to the vertex mapping method employed in [23] (but with some necessary modifications). Briefly, for any vertex $X_i \in \mathrm{M}$, we determine its closest woven node $V_{i,j}$ on Γ by a local searching. The local searching can be finished in a very short time since in the data-structure of every polygonal face there is a pointer linking to the woven nodes lying on the face (see [23]). After that, a weft unit vector t_{weft} is formed by either $V_{i+1,j}V_{i,j}$ or $V_{i-1,j}V_{i,j}$ – choosing $V_{i+1,j}V_{i,j}$ or $V_{i-1,j}V_{i,j}$ depends on the sign of the projection of $X_iV_{i,j}$ on $V_{i+1,j}V_{i,j}$ (i.e., $V_{i+1,j}V_{i,j}$ if it is positive, and $V_{i-1,j}V_{i,j}$ for negative). In a similar manner, a unit warp vector t_{warp} is formed by either $V_{i,j+1}V_{i,j}$ or $V_{i,j-1}V_{i,j}$. In case $V_{i,j}$ is a boundary woven node, some of $V_{i\pm1,j}V_{i,j}$ and $V_{i,j\pm1}V_{i,j}$ might not exist; then, the existing one will be taken as the row or column vector. In the worst case, $V_{i,j}$ has neither $V_{i+1,j}V_{i,j}$ nor $V_{i-1,j}V_{i,j}$ neighbor, or neither $V_{i,j+1}V_{i,j}$ nor $V_{i,j-1}V_{i,j}$ neighbor, then we have to use other woven node to perform the vertex mapping. The projections of $X_iV_{i,j}$ on t_{warp} and t_{weft} are $\langle X_iV_{i,j}, t_{warp}\rangle$ and $\langle X_iV_{i,j}, t_{weft}\rangle$. Therefore, by keeping the same ratio of their lengths on 3D and 2D, the planar coordinate of X_i can be determined by

$$x_i = L_{warp}\left[j \pm \langle X_iV_{i,j}, t_{warp}\rangle / \|V_{i,j}V_{i,j\pm1}\|\right] \tag{8}$$

$$y_i = L_{weft}\left[i \pm \langle X_iV_{i,j}, t_{weft}\rangle / \|V_{i,j}V_{i\pm1,j}\|\right] \tag{9}$$

where the sign $\pm$ is determined by the direction of $X_iV_{i,j}$. An illustration of this interpolation is shown in Fig.5.

5. Algorithmic Details

As alluded, the exact placement of the warp threads on M is obtained through an energy diffusion process that minimizes the energy J_E of Eq. (4), with Eqs. (5-7) incorporated. The overall algorithm consists of three steps:

1. Compute the initial planar shape Ω of the given mesh M by the intrinsic parameterization [5], which gives the initial fitting of the woven model Γ;

Do {

2. Determine the expected strain of every weft and warp spring on Γ;
3. Move the woven nodes on the surface of M through energy diffusion;

} *WHILE* (the terminal condition has Not been reached);

The details are given next.

5.1. *Strain distribution fitting*

The normal pressure assigned by a physician is specified only at some discrete points on the mesh surface M, which may not coincide exactly with the woven nodes during the diffusion. At the beginning of Step 2, for every point with a prescribed

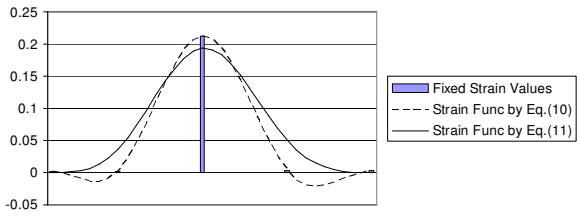

Fig. 6. An example of strain distribution function with three fixed warp strains.

normal pressure we locate its closest woven node on M and assign that normal pressure to the located woven node. Then, Eq.(3) is invoked to calculate the strains on all the warp threads which have at least one such located node. The remaining issue in strain calculation is to obtain the warp strain distribution function $\varepsilon(t)$ that will interpolate for those warp threads not containing any such located nodes. The function $\varepsilon(t)$ should be smooth and flat at the two ends (i.e., $\varepsilon'(0) = 0$ and $\varepsilon'(1) = 0$). In addition, we only want to have tensile strains; that is, $\varepsilon(t) \geq 0$ for all $t \in [0,1]$. This is a typical curve interpolation problem. For the given data points ε_j at their corresponding parameters t_j ($j = 1, \cdots, l$), a B-spline interpolation is

$$\varepsilon(t) = \sum_{i=0}^{n-1} Q_i N_{i,3}(t) \tag{10}$$

which interpolates all the ε_j s together with the constraints $\varepsilon'(0) = 0$ and $\varepsilon'(1) = 0$, where Q_i s are the control points and $N_{i,3}(t)$ s are the B-spline basis functions of degree 3. Details in B-splines can be found in [27] or any texts on B-spline curves. To ensure that $\varepsilon(t) \geq 0$ for all t, we instead use

$$\varepsilon(t) = \sum_{i=0}^{n-1} Q_i^2 N_{i,3}(t) \tag{11}$$

which guarantees $\varepsilon(t) \geq 0$ since $N_{i,3}(t) \geq 0$ and $Q_i^2 \geq 0$. Note that when $l > 1$, we adopt $n = l + 2$ control points; when $l = 1$, we use four control points $Q_i \equiv \sqrt{\varepsilon_1}$ ($i = 0, \cdots, 3$). However, it may happen (though rarely) that the curve in the form of Eq.(11) is unable to interpolate all the given data points. In such a case, we use Eq.(10) and simply floor the negative function values by zero.

5.2. *Diffusion of elastic energy*

The movement of woven nodes at Step 3 is governed by the elastic energy function defined in Eq. (4), together with Eqs.(5-7). To minimize J_E, one should let every node V in the woven model Γ satisfy

$$\frac{\partial J_E}{\partial V} = \sum_{j \in N(V)} k_j \frac{VV_j}{\|VV_j\|} \left(\|VV_j\| - L_{S_j} \right) = 0 \tag{12}$$

where $N(V)$ represents the 1-ring neighbors of V, i.e. those with a spring linked to V. A diffusion process similar to that of [28] is used to solve Eq.(12). Taking the current $\partial J_E / \partial V$ as a force in a spring-mass system, the new position of V is computed by

$$V^{new} = V - \lambda \frac{\partial J}{\partial V} \tag{13}$$

where λ is a damping factor to control the movement of V in every iteration. This diffusion process is similar to the quasi-Newton type numerical optimization scheme. Here the movement of woven node V is along the geodesic path determined by $\partial J_E / \partial V$ with distance $\lambda \| \partial J_E / \partial V \|$. Choosing a smaller λ will lead to more accurate results but at the cost of a slower diffusion speed, while using a large λ may make the system become unstable. We use $\lambda = 0.125 / \max\{k_{warp}, k_{weft}\}$ in all our tests and find it to work well. We adopt the method introduced in [29] to compute the discrete geodesic path following a given direction vector t_0 on a given mesh surface at a point p_0. The algorithm is in fact a local incremental approach. At every point pi on the mesh, the geodesic path is locally coincident to the intersection curve the plane formed by p_i, t_i and n_i, where n_i is the mesh surface normal at p_i and t_i is the tangent of the geodesic path at this point.

In the diffusion process, the overall orientation of the woven threads on M may become twisted in some sense. This is undesirable from a physician's point of view. As a solution to this problem, in the beginning of the diffusion we ask the user to specify two points on M as two orientation markers. After every iteration of Step 2 & 3, we check the corresponding planar mapping points of the two markers. If the two do not lie on a vertical line, we will rotate all the planar vertices to align the two corresponding points to a vertical line.

Also, during the diffusion, some nodes may move beyond the boundary of M ; if so, these nodes together with the springs linked to them are removed from Γ. On the other hand, new nodes will often need to be inserted into M , if some gap emerges near the boundary of M .

Another issue related to the diffusion of elastic energy is the selection of initial values. Similar to most other numerical optimization techniques, the result of our energy diffusion relies heavily on the given initial values. From our investigation, we find that, similarly to other spring systems, it is easier for our system to converge when the springs are deformed from the tensile state back to the rest state, as compared to the opposite, i.e., from the compressed state to the rest state. Therefore, at Step 1 of the overall algorithm, after obtaining the intrinsic parameterization (which is close to a stretch-free state), we scale down the planar coordinates of all the vertices with some ratio r ≤ 1, in both vertical and horizontal directions. As a result, most springs in the woven model after Step 1 are in the tensile state. In our implementation, we set r to 0.75 in the warp direction, and 1 in the weft direction (i.e., the woven threads in weft direction are unaffected).

5.3. *Error measurement and terminal condition*

The iterative diffusion algorithm needs certain error measurement to evaluate the convergence of the iteration. In our approach, we measure the squared strain difference (SSD) on the fitted woven model. For all warp and weft springs (we exclude diagonal springs as their contribution to the normal

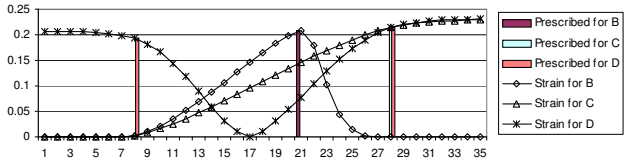

Fig. 7. The strains (in bar-chart) determined from prescribed normal pressures and the strain distribution function curve interpolating the strains for three different normal pressure configurations (B, C and D) on the elbow brace example shown in Fig.2. As no normal pressure is assigned for the configuration A, its warp strain function is a constant zero.

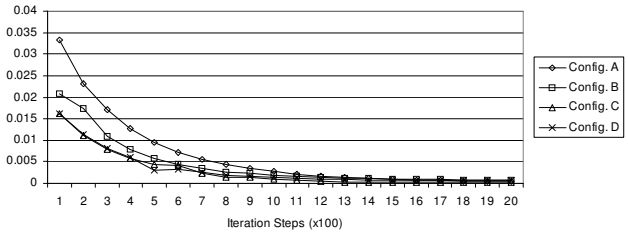

Fig. 8. The E_{SSD} curve of the elbow brace with four different normal pressure configurations in test example 1.

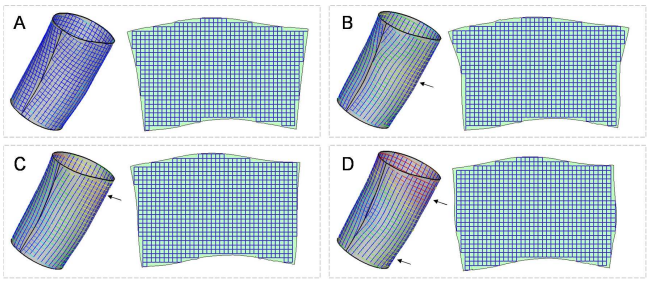

Fig. 9. The flattened planar patterns of an elastic elbow brace corresponding to four different normal pressure configurations, with drastically different warp and weft stiffness. The places pointed by arrows are with large normal pressures specified.

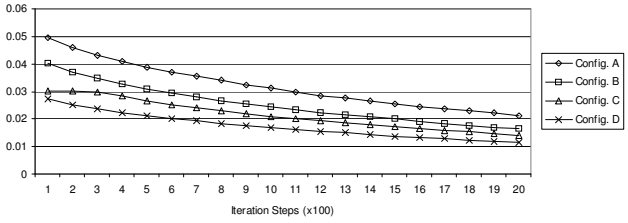

Fig. 10. The E_{SSD} curve of the elbow brace in test example 2 shown in Fig. 9.

pressure is ignored due to Lemma 2), the SSD is defined as

$$E_{SSD} = \sum_S (\varepsilon_S - \varepsilon_S^0)^2 \qquad (14)$$

where ε_S is either ε_{warp} or ε_{weft} depending on the type of the spring and ε_S^0 is the desired strain on the spring. An empirical threshold E_{SSD}^0 is used to determine the termination of the iteration: the diffusion will continue if $E_{SSD} > E_{SSD}^0$, unless a pre-set maximum number of iterations is reached.

6. Numerical Results

A prototype of the proposed woven fitting algorithm has been implemented using C++. Several examples are tested and given below to demonstrate the proposed method.

The first example is the one that has been previously shown in Fig.2 – this is a medical assistive brace for elbow. Based on the triangular mesh and its initial intrinsic parameterization (see Fig.2(a)), we use our approach to generate the planar patterns for four different normal pressure configurations:

- Configuration A) – no normal pressure is assigned and the fitting result minimizes the stretch (see top-left in Fig.2(b)); often this is called stretch-free although it is not really "stretch-free" in general.
- Configuration B) – large normal pressure is specified in the middle of the brace while a very small normal pressure is assigned at the two ends of the brace; the result pattern leads to a tighter stretch in the middle of the brace (see top-right in Fig.2(b)).
- Configuration C) – large normal pressure is assign at one end of the brace while a very small one is specified at the other end; the final brace has large stretch on one side while almost stretch free on the other (see bottom-left in Fig.2(b)).
- Configuration D) – large normal pressure is assigned at two ends of the brace; the result is depicted in the bottom-right part in Fig.2(b), which shows almost no stretch in the middle part of the brace.

The strain distribution function for warp springs generated by the last three configurations is given in Fig.7, where the strains determined by user-specified normal pressures are represented by bar-charts. The strain distribution function curve is computed by interpolating these strain values. Fig.8 shows the E_{SSD} as a function of iterations during the diffusion for the four configurations. The spring stiffness coefficients adopted in this test are k_{warp}=0.5, k_{weft}=0.5, and k_{diag}=0.05, which simulate a woven fabric with similar strengths in both directions.

The second example also simulates the woven fitting of an elbow brace, but with anisotropic material this time. By observation, owing to the fact that the geometry of a human joint is more or less cylindrical with a large disparity between the curvatures in the "radial" (warp) and "axial" (weft) directions, in most cases it is much harder to stretch along the weft direction than the warp direction (i.e., $k_{weft} >> k_{warp}$)[2]. To reflect this nature, we choose k_{warp}=0.5, k_{weft}=5.0, and k_{diag}=0.05. The second test example conducts the similar normal pressure configurations but with different amplitudes. The obtained fitting results and their corresponding planar patterns are shown in Fig. 9, and Fig. 10 displays the corresponding E_{SSD} during the diffusion process. Comparing Fig. 8 and Fig. 10, it is noted that the diffusion process converges faster in the "isotropic" case ($k_{weft} \approx k_{warp}$) than in the "anisotropic" case ($k_{weft} >> k_{warp}$). This is not unexpected, since stiff weft threads (when $k_{weft} >> k_{warp}$) reduce the degree of

[2] In the case of elbow or ankle braces, this is purposely designed as no shrinkage is wanted in the "axial" (weft) direction.

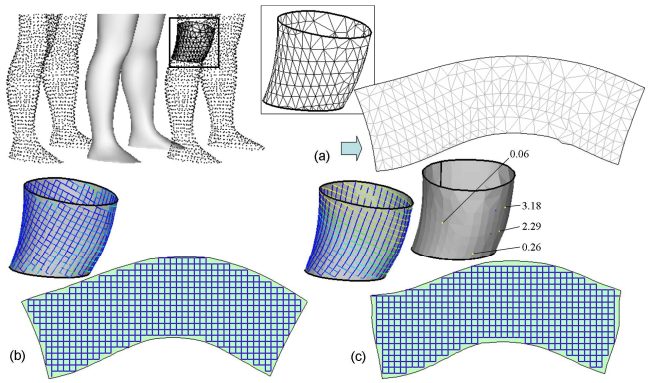

Fig. 11. Geometric design of a knee brace: (a) the 3D geometry of the knee joint obtained by laser scanning, and the initial pattern determined by the intrinsic parameterization [5]; (b) the computed woven fitting and its corresponding planar pattern without prescribed normal pressure; (c) the result with normal pressures specified at four points.

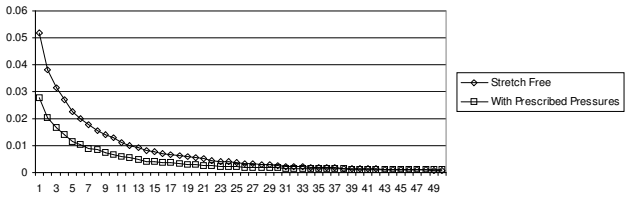

Fig. 12. The E_{SSD} curve of the knee brace with and without normal pressure constraints.

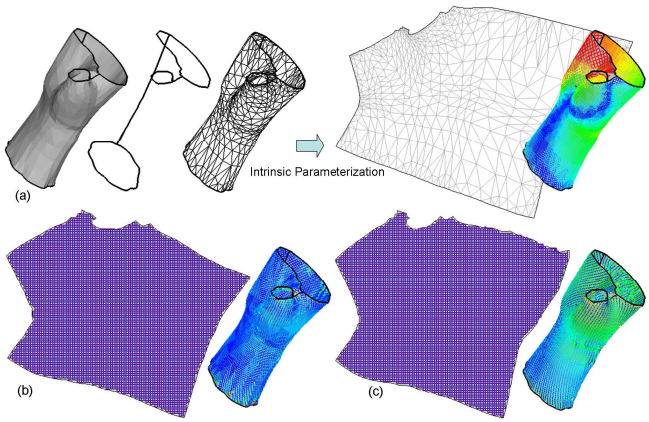

Fig. 13. The geometric design for a wrist brace: (a) the 3D mesh surface of the wrist, the initial woven fitting of the wrist, and the corresponding strain distribution of the brace; (b) the fitting result without normal pressure constraints; (c) the fitting result with normal pressure constraints.

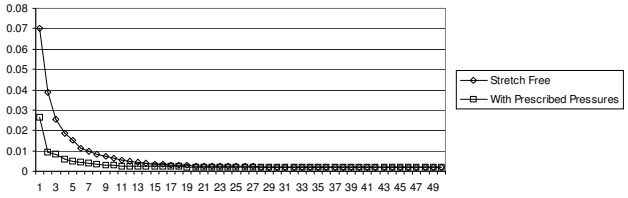

Fig. 14. The E_{SSD} curves of the wrist brace with and without normal pressure constraints.

move-ability of nodes on M.

Our third example is a medical assistive brace for a knee joint. Similar to example 1 and 2, the geometry of the knee joint is acquired via 3D laser scanning on a human model. After constructing the 3D triangular mesh for the knee brace, we apply the intrinsic parameterization [5] to determine the initial shape of the planar pattern (see Fig.11(a)). Then, we fit the woven model on the 3D mesh surface with (Fig.11(c)) and without (Fig.11(b)) normal pressure constraints. The normal pressure constraints are given at four sample points, with assigned values 0.06, 3.18, 2.29, and 0.26 respectively (see Fig.11(c)). Anisotropic material is chosen for the brace with k_{warp}=0.5, k_{weft}=5.0, and k_{diag}=0.05. From the results in Fig.11(c), we find that it is impossible to realize the two drastically different normal pressures at two points (i.e., the point with pressure 2.29 and the point with 0.06) which have similar curvature and are close in the weft direction (though they are far from each other in the warp direction). Fig.12 displays the corresponding E_{SSD} curves.

The last test example is one with more complex geometry – a wrist brace (see Fig.13). The presented woven fitting algorithm is tested for both cases with and without normal pressure constraints, with a material setting of k_{warp}=0.75, k_{weft}=0.5, and k_{diag}=0.05. For the case with normal pressure assignment, high normal pressure is specified near the bottom of the thumb. As seen in the colored strain distribution figure in Fig. 13(a), the initial fitting incurs very high distortion (twice that of previous examples). Fig. 13(b) shows the fitting result for the case without normal pressure assignment, with a much lowered strain distribution; and that with the prescribed normal pressure is depicted in Fig. 13(c). The corresponding E_{SSD} curves for both cases are given in Fig. 14.

7. Summary and Discussion

This paper presents a novel method for the geometric design of customized elastic medical braces that preserve prescribed normal pressures. The core of the method is a woven fitting algorithm that finds a suitable mapping between the 3D surface of the brace and its relaxed 2D pattern, with the prescribed normal pressure constraints respected. The normal pressure constraints are first converted into a corresponding strain distribution, and an elastic energy diffusion process is then used to determine the positions of woven nodes on the 3D surface, with the minimum state of the energy system corresponding to the best fitting respecting the required strain distribution. Finally, through an interpolation scheme, the obtained node-only discrete surface-plane mapping is extended to a continuum mapping. In summary, our work bears several key points:

- No similar work has been found in the literature about the computer-aided geometric design of elastic medical braces. Our analytical and algorithmic work provides a needed effort in addressing this important problem.
- Preliminary experiments of our implemented system show positive results, indicating that it offers to be a useful and practical tool for automating the design task,

which is currently carried out in an ad-hoc and trial-and-error manner.

- The methodology developed by us can also benefit other industrial applications that have similar surface flatting requirement, e.g., the garment industry, the design of footwear, and the design and manufacturing of furniture.

However, this is only an initial study. Many issues and questions remain, of which we are particularly interested in the following and plan to further our study in them:

- In the current implementation, we use simplified formulae, Eq. (1) & (2), to locally relate the normal pressure to the tensile strains. More investigation, in both theoretical study and physical experiments, is required to validate our formulation.
- From our preliminary experiments, in the form of both computer simulation and physical experiments, we found that the distribution of normal pressure on the joint by a brace heavily depends on the geometry of the joint – the curvature of the surface plays a crucial role in normal pressure distribution. When the geometry of the joint is simple with little curvature variation, it appears that the freedom of achieving diverse normal pressure distributions is severely limited, no matter what the 2D pattern is (e.g., example in Fig. 11(c)). Systematic study is needed in understanding the global relationship between the two.
- The friction between the brace and the surface of the joint is completely ignored in our model. This simplification leads to our assertion that the strain in any warp thread is a constant, which in turn helps tremendously reduce the complexity of the formulation. While this assumption seems to agree with our observation of braces – the fitting configuration of the brace due to the friction is extremely unstable and the final stable fitting of the brace appears to be always in a minimum strain energy state, we need to look into situations when this supposition might no longer be valid, such as the case of very large normal pressure.
- Some material related coefficients (e.g., s in Eq.(1)) need to be determined by experimental tests, where certain specialized equipments like *Kawabata System* [30] need to be developed.
- The research in this paper concentrates on that different braces may have various effects under the same bending situation on the same person. A possible dynamic research can extend the current work to analysis the effects of different braces have different forces on body surface when they are bent in different angles.

Finally, it is necessary to note that our method applies only to woven-like materials. For isotropic materials, different geometric formulations have to be established and new surface flattening algorithm needs to be developed.

REFERENCES

[1] I. Atroshi, and C. Gummesson, "Prevalence of carpal tunnel syndrome in a general population," *Journal of American Medical Association*, vol.282, no.2, pp.153-158, 1999.

[2] Cyberware, http://www.cyberware.com.

[3] Paraform, http://www.paraform.com.

[4] $[TC]^2$, http://www.tc2.com/what/bodyscan/index.html.

[5] M. Desbrun, M. Meyer, and P. Alliez, "Intrinsic parameterizations of surface meshes," *Eurographics 2002*, *Computer Graphics Forum*, vol.21, no.3, pp.209-218, 2002.

[6] T.D. Yoo, E. Kim, J.H. Han, and D.K. Bogen, "Geometric and biomechanical analysis for computer-aided design of assistive medical devices," *Computer-Aided Design*, vol.37, no.14, pp.1469-1480, 2005.

[7] M.S. Floater, and K. Hormann, "Recent advances in surface parameterization," In *Multiresolution in Geometric Modeling*, pp.259-284, 2003.

[8] M.S. Floater, "Parametrization and smooth approximation of surface triangulations," *Computer Aided Geometric Design*, vol.14, no. 3, pp.231-271, 1997.

[9] B. Levy, S. Petitjean, N. Ray, and J. Maillot, "Least squares conformal maps for automatic texture atlas generation," *SIGGRAPH 2002*, *ACM Transactions on Graphics*, vol.21, no.3, pp.362-71, 2002.

[10] A. Sheffer, and E. de Sturler, "Parameterization of faceted surfaces for meshing using angle based flattening," *Engineering with Computers*, vol.17, no.3, pp.326-337, 2001.

[11] A. Sheffer, and E. de Sturler, "Smoothing an overlay grid to minimize linear distortion in texture mapping," *ACM Transactions on Graphics*, vol.21, no.4, pp.874-890, 2002.

[12] P.V. Sander, J. Snyder, S.J. Gortler, and H. Hoppe, "Texture mapping progressive meshes," *SIGGRAPH 2001 Conference Proceeding*, pp.409-416, 2001.

[13] S. Yoshizawa, A. Belyaev, and H.P. Seidel, "A fast and simple stretch-minimizing mesh parameterization," *International Conference on Shape Modeling and Applications 2004*.

[14] C. Bennis, J.M. Vezien, and G. Iglesias, "Piecewise surface flattening for non-distorted texture mapping," *ACM SIGGRAPH Computer Graphics*, vol.25, no.4, pp.237-246, 1991.

[15] P.N. Azariadis, and N.A. Aspragathos, "Design of plane development of doubly curved surface," *Computer-Aided Design*, vol.29, no.10, pp.675-685, 1997.

[16] J. McCartney, B.K. Hinds, and B.L. Seow, "The flattening of triangulated surfaces incorporating darts and gussets," *Computer-Aided Design*, vol.31, pp.249-260, 1999.

[17] J. McCartney, B.K. Hinds, B.L. Seow, and D. Gong, "An energy based model for the flattening of woven fabrics," *Journal of Materials Processing Technology*, v.107, pp.312-318, 2000.

[18] P.N. Azariadis, and N.A. Aspragathos, "Geodesic curvature preservation in surface flattening through constrained global optimization," *Computer-Aided Design*, vol.33, no.8, pp.581-591, 2001.

[19] C.C.L. Wang, S.S.F. Chen, and M.M.F. Yuen, "Surface flattening based on energy model," *Computer-Aided Design*, vol.34, no.11, pp.823-833, 2002.

[20] M. Aono, D.E. Breen, and M.J. Wozny, "Fitting a woven-cloth model to a curved surface: mapping algorithms," *Computer-Aided Design*, vol.26, no.4, pp.278-292, 1994.

[21] M. Aono, P. Denti, D.E. Breen, M.J. Wozny, "Fitting a woven cloth model to a curved surface: dart insertion," *IEEE Computer Graphics & Applications*, vol.16, no.5, pp.60-70, 1996.

[22] M. Aono, D.E. Breen, and M.J. Wozny, "Modeling methods for the design of 3D broadcloth composite parts," *Computer-Aided Design*, vol.33, no.13, pp.989-1007, 2001.

[23] C.C.L. Wang, K. Tang, and B.M.L. Yueng, "Freeform surface flattening based on fitting a woven mesh model," *Computer-Aided Design*, vol.37, pp.799-814, 2005.

[24] N.E. Dowling, *Mechanical Behavior of Materials*. New York: Prentice-Hall, 1993.

[25] Y.C. Fung, *Foundations of Solid Mechanics*. Englewood Cliffs, N.J.: Prentice-Hall, 1965.

[26] M. Meyer, M. Desbrun, P. Schroder, and A. H. Barr, "Discrete differential-geometry operators for triangulated 2-manifolds," *Proceeding of Visualization and Mathematics*, 2002.

[27] L. Piegl, and W. Tiller, *The NURBS Book*. Berlin; New York: Springer, 1995.
[28] M. Desbrun, M. Meyer, P. Schröder, and A. Barr, "Implicit fairing of irregular meshes using diffusion and curvature flow," *Proceedings of SIGGRAPH 99*, pp.317-324, 1999.
[29] G.V.V. Ravi Kumar, P. Srinivasan, V. Devaraja Holla, K.G. Shastry and B.G. Prakash, "Geodesic curve computations on surfaces," *Computer Aided Geometric Design*, vol.20, no.2, pp.119–133, 2003.
[30] *Kawabata Evaluation System for Fabrics*, http://www.kod.vslib.cz/laboratore/Kes/index_eng.html.